

Increased flow speed on a large East Antarctic outlet glacier caused by subglacial floods

LEIGH A. STEARNS^{1*}, BENJAMIN E. SMITH² AND GORDON S. HAMILTON¹

¹Climate Change Institute, University of Maine, 5790 Bryand Global Science Center, Orono, Maine 04469, USA

²Applied Physics Laboratory, University of Washington, 1013 NE 40th Street, Seattle, Washington 98105, USA

*e-mail: leigh.stearns@maine.edu.

Published online: 16 November 2008; doi:10.1038/ngeo356

Changes in the velocity of large outlet glaciers and ice streams in Greenland and Antarctica are important for ice-sheet mass balance and hence sea level¹. Mass loss in large parts of both ice sheets is being driven by the recent accelerations of outlet glaciers^{2–5} in response to unknown or poorly constrained climatic or internal perturbations in their boundary conditions. Surprisingly active networks of subglacial lake drainage have recently been found beneath the Antarctic ice sheet and tentatively linked to the onset of fast ice flow^{6–8}. Here we report an observed acceleration of ice velocity on Byrd Glacier, East Antarctica, of about 10% of the original speed between December 2005 and February 2007. The acceleration extended along the entire 75 km glacier trunk and its onset coincided with the discharge of about 1.7 km³ of water from two large subglacial lakes located about 200 km upstream of the grounding line. Deceleration coincided with the termination of the flood. Our findings provide direct evidence that an active lake drainage system can cause large and rapid changes in glacier dynamics.

The causes of rapid changes in outlet glacier flow speed are not fully understood. Whereas fluctuations in Greenland glacier velocities are thought to be driven in part by water infiltrating from extensive surface meltwater and lakes^{9–11}, velocity changes of Antarctic outlet glaciers are thought to result from sub-ice-shelf melting at marine margins and a subsequent reduction in buttressing¹². Because East Antarctica is too cold to experience sustained summer melting, surface meltwater production is not a likely cause of changes in outlet glacier dynamics. Water, however, might still have an important role. Subglacial lakes are common in Antarctica¹³, and although many lakes are located beneath domes and ice divides⁷, others have a close geographic association with outlet glaciers and ice streams^{6,8,14}. Recent satellite-altimeter mapping of elevation changes indicates that water from some subglacial lakes can move rapidly and over long distances via interconnected drainage networks^{7,8}. An active subglacial drainage system provides a mechanism for quickly perturbing basal boundary conditions and suggests that the motion of lake water can modify outlet glacier dynamics but, until now, no direct evidence has supported this hypothesis.

Byrd Glacier (80.5° S, 160° E) has one of the largest catchment basins in Antarctica (1,070,400 km²), and funnels 20.6 ± 1.6 Gt yr⁻¹ (ref. 15) of ice to the Ross Ice Shelf through a ~75-km-long, ~20-km-wide fjord. Because of its size, the glacier exerts a

potentially important control on the mass balance of the East Antarctic ice sheet and hence sea level. Its large flux, amounting to ~18% of the total ice inflow to the Ross Ice Shelf¹⁶, probably has a role in the ice shelf's stability. Here, we report new remote-sensing measurements of ice velocity for the trunk of Byrd Glacier acquired between 1988 and 2008 (Fig. 1).

Velocities are derived from automatic tracking of surface crevasses on sequential satellite images using a cross-correlation technique¹⁷. We use numerous image pairs (see Supplementary Information, Table S1) acquired by several optical imaging satellites to produce a detailed time series of velocity patterns. Ground-based measurements collected in 1960–1961 (ref. 18) and photogrammetric measurements in 1978–1979 (ref. 19) provide a longer-term perspective on the glacier's flow.

The 48-year record of ice velocity (Fig. 1a) shows no detectable change in speed along the grounded trunk of Byrd Glacier between November 1960 and December 2005. Speeds at the inferred grounding line (at $x \approx 25$ km in Fig. 1) during this period were ~825 m yr⁻¹, decreasing to ~450 m yr⁻¹ some 50 km inland. After December 2005, the lowermost ~100 km of the glacier trunk began to accelerate (Fig. 1a, b). The acceleration continued until February 2007, amounting to a ~10% speed-up along the entire length of the trunk, and an increase in mass discharge from 20.6 ± 1.6 Gt yr⁻¹ (before 2005) to 22.3 ± 1.7 Gt yr⁻¹ (in 2006) (ref. 15).

Peak speeds were reached between December 2005 and February 2007, with the fastest velocities (~900 m yr⁻¹) observed near the grounding line. Close examination of the image pairs (Fig. 1a) enables us to further constrain the timing. The difference in velocity between image pairs that end in December 2006 (~850 m yr⁻¹) and those that end in January/February 2007 (~890 m yr⁻¹) suggests that peak speeds occurred in a short period in late 2006 or early 2007. The glacier decelerated between February 2007 and January 2008, but was still moving faster than pre-speed-up values (Fig. 1a). These observations indicate the acceleration was a sudden and short-lived event.

The observed speed-up coincides with rapid changes in surface elevation at two locations ~200 km upstream of the grounding line detected using laser altimeter data from NASA's Ice, Cloud and land Elevation Satellite (ICESat). Altimeter measurements were chosen among 12 separate 33-day campaigns between August 2003 and November 2007, and processed (see the Methods section) in a repeat-track analysis^{8,20}.

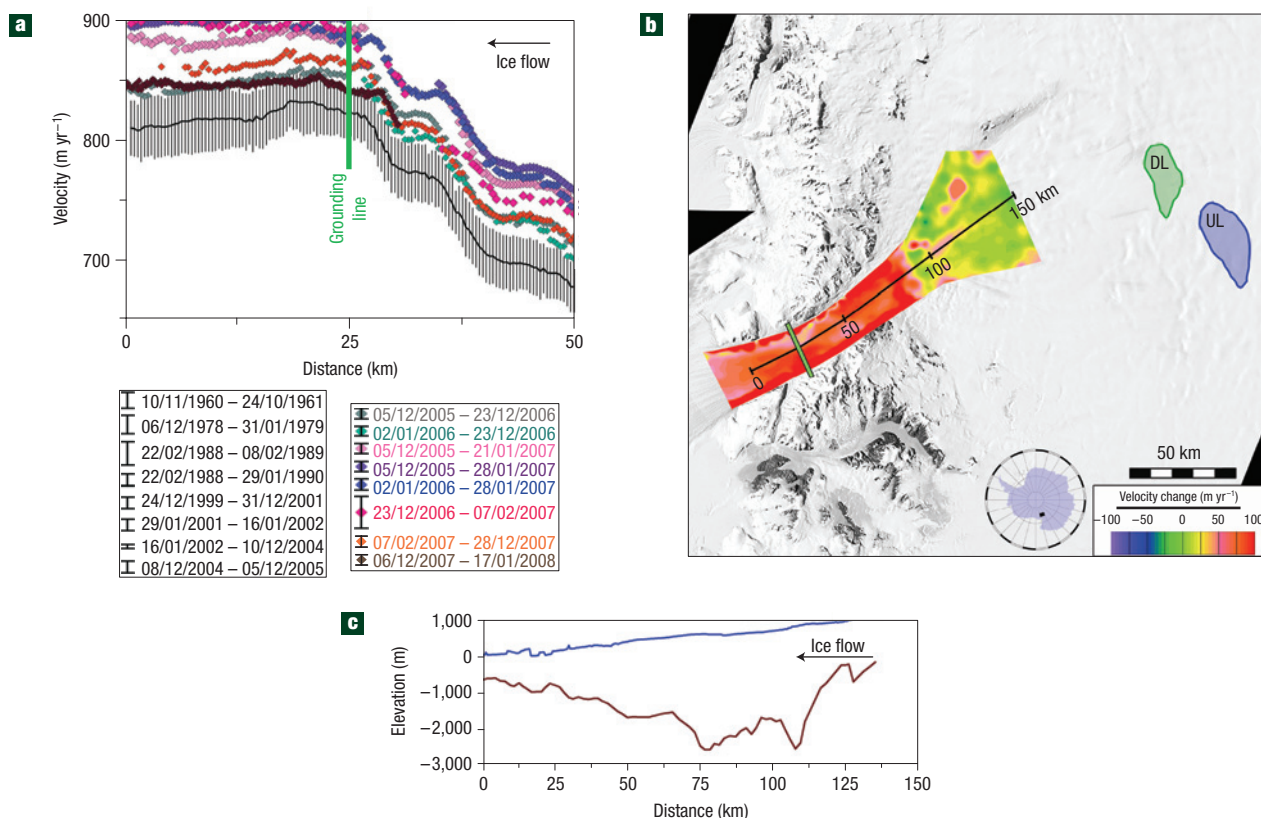


Figure 1 Byrd Glacier ice velocity. **a**, Ice velocity along a portion of the profile in **b** derived from repeat geodetic measurements in 1960–1961 (ref. 18), photogrammetry in 1978–1979 (ref. 19) and feature tracking on optical satellite images. The black line represents the mean of pre-2005 ice velocities; the thin vertical lines represent the standard deviation of all pre-2005 velocities. Errors associated with each measurement epoch are shown in the lower boxes and are derived from procedures described in the Methods section. **b**, A contour map of velocity change (in m yr^{-1}) derived from pre-2005 average speeds and peak speeds during 2006–2007, overlain on a Landsat image. The grounding line^{15,19} is shown in green, which is at $x \approx 25$ km in **a** and **c**. Outlines of the inferred subglacial lakes are shown in green (downstream lake, DL) and blue (upstream lake, UL). **c**, Surface elevation (blue line) from the ICESat DEM²⁴ and bed topography from a 1978–1979 airborne survey²⁷.

There are two discrete regions in the Byrd Glacier catchment where surface elevations varied by up to 12 m (Fig. 2a,b) over the 4.2-year ICESat time period. For each epoch, the spatial pattern of elevation change was consistent for these discrete regions (Fig. 2b), varying smoothly on scales of ~ 10 km. The elevation changes seen here are far outside the range of ICESat elevation changes (usually < 0.1 m) detected in most parts of Antarctica, but are similar to other regions where elevation changes of several metres have been interpreted as the filling and draining of subglacial lakes⁸. We infer that these regions overlie subglacial lakes, and that their motion reflects filling and emptying of the lakes.

The temporal and spatial sampling of the lakes is coarse. ICESat observations are repeated every 4–6 months, with about 13 km separating the adjacent tracks (Fig. 2c). However, fitting a smooth surface to the elevation residuals for each period enables a rough estimate of the water volume displaced; a precise volume estimate is impossible to obtain because some of the elevation change is due to unknown local ice flow effects resulting from lake infilling and draining²¹. Figure 2c shows the range of surface elevations for the fitted surfaces at each elevation-change region. The gridded volume estimates (Fig. 2d) show that the upstream lake gained 1.4 km^3 between November 2003 and November 2005, then lost a similar amount between November 2005 and April 2007. The downstream lake gained 1.7 km^3 between March 2004 and June 2006, then lost 1 km^3 between June 2006 and March 2007, and refilled between

March 2007 and November 2007. It seems that the downstream lake followed the same volume history as the upstream lake, but lagged by approximately 0.6 years. Adding the volume displacements for the two areas gives a net gain of 2.1 km^3 between March 2004 and November 2005, followed by a loss of 1.7 km^3 between June 2006 and April 2007, with minor refilling between April and November 2007. On the basis of the volume loss and its duration, we estimate a peak discharge rate of $\sim 70 \text{ m}^3 \text{ s}^{-1}$ during the flood.

Figure 2d,e shows the timing of lake volume change and ice acceleration. The 0.6-year lag in the filling and draining of the downstream lake relative to the upstream lake suggests that a pulse of water moved through the system reaching the upstream lake on or before November 2003. Sometime between November 2003 and March 2004, the downstream lake began to fill as well, which may reflect a water transfer between the lakes, or may show that by this time they were both connected to the same active drainage network. The upstream lake began to drain in November 2005, whereas the downstream lake was still filling; the downstream lake began to drain around June 2006. The peak lake discharge occurred between March 2006 and February 2007. By mid-2007, both lakes were refilling.

Within the temporal resolution of the data, the velocity changes of Byrd Glacier coincided with the lake discharge events. The onset of glacier acceleration, the peak speed and subsequent deceleration coincided with the start of drainage, the maximum discharge and the end of drainage, respectively (Fig. 2d,e).

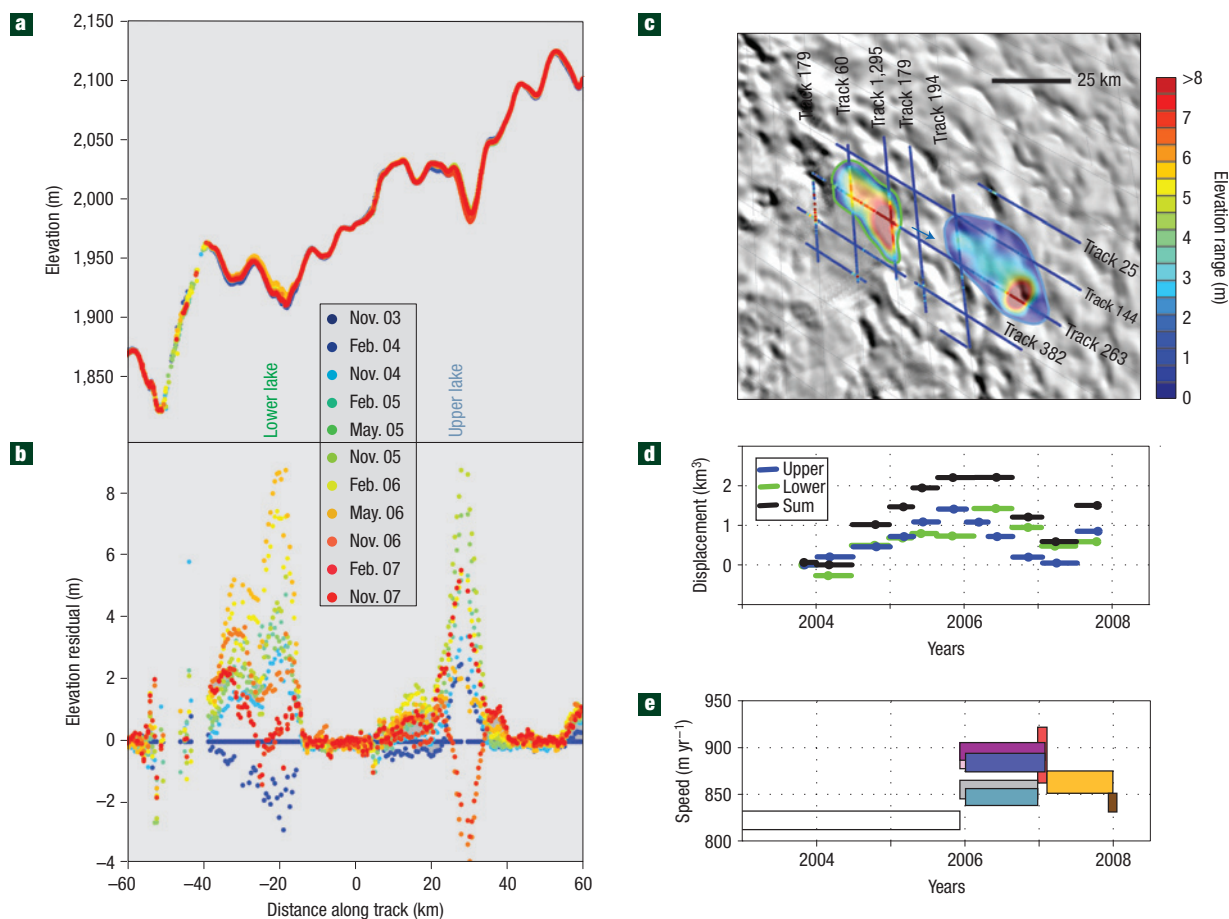


Figure 2 Surface elevation change. **a**, ICESat elevations for 11 passes over reference track 263, between November 2003 and November 2007. **b**, Elevation residuals for ICESat data after correction for topography. **c**, Map of elevation ranges for 500 m sections of track, interpreted lake boundaries (green, blue outlines) and elevation ranges for gridded surface displacements, overlaid on a Moderate Resolution Imaging Spectroradiometer image mosaic²⁸. The arrow indicates the direction and orientation of the profiles in **a** and **b**. The colour scale gives displacement magnitudes; the colours in the figure are semi-transparent and may be slightly different from those in the colour scale. **d**, Estimated lake volume displacements for the downstream lake (green), the upstream lake (blue) and the two lakes together (black). The horizontal bars show time-uncertainty in lake volumes. **e**, Ice speed at the grounding line from 2003 to 2008. The horizontal bars indicate start and end dates for each pair of observations; the thickness of each bar represents its associated error; the colours are the same as in Fig. 1a.

The exact path of water drainage is not known, but calculations of the relative hydraulic pressure²² of the Byrd catchment using gridded maps of ice thickness³³ and surface elevation²⁴ show that subglacial pressure at the lakes was $\sim 15,000$ kPa higher than at the grounding line (Fig. 3). The hydraulic pressure contours show that water was capable of flowing from the upstream lake to the downstream lake, although it is also possible that some water diverted around the downstream lake, depending on the location of the lake outlet. Regardless of the exact path, the steep surface slope and constrained fjord of Byrd Glacier makes drainage towards the glacier trunk and ice shelf likely.

The subglacial hydrological characteristics of Antarctic glaciers are almost entirely unknown, but our observations enable us to infer those characteristics for Byrd Glacier. Flow lines converge to form the main trunk of Byrd Glacier at $x \approx 100$ km in Fig. 1a. This location corresponds to a rapid deepening of the glacier trough (Fig. 1c), the onset of very fast velocities (>400 m yr⁻¹) and the upstream limit of the 2005–2007 speed-up event (Fig. 1a). These observations point to a change in basal hydrological characteristics at this location. We propose that water upstream of the transition is transported through a channel-dominated drainage system²², whereas downstream, water is carried in a distributed network

of smaller drainage conduits similar to a linked-cavity drainage system hypothesized to exist beneath actively surging glaciers²⁵. The large driving stresses (>200 kPa) of Byrd Glacier are predominantly resisted by basal drag concentrations^{15,26} ('sticky spots'). As the lakes drain, the distributed drainage network downstream of the deepening is unable to discharge the incoming water, and subglacial water volumes steadily increase to submerge a larger fraction of the glacier bed. Submergence of the sticky spots reduces basal friction and promotes faster ice velocities. Conversely, as lake drainage decreases, more of the sticky spots are exposed as the distributed drainage system approaches a new discharge equilibrium, and the glacier decelerates.

Our time series of surface elevation changes is too short, and the velocity time series too sporadic before 2000, to tell if the sequence of lake filling and draining is a cyclical or discrete event. If cyclical, the return interval must be longer than ~ 5 years, because we do not detect any other period of glacier acceleration between 2000 and 2007. Other studies of active subglacial lakes elsewhere in Antarctica have yielded multi-decadal return periods⁷ or revealed no evidence of cyclicity⁸.

Our study shows that the flow of large East Antarctic outlet glaciers can change rapidly in response to non-climatic

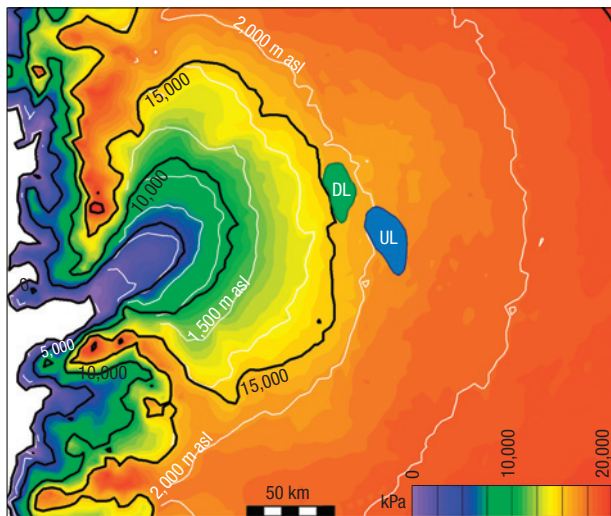


Figure 3 Hydraulic pressure. The black contours show hydrostatic pressure (relative to pressure at the grounding line) at the base of Byrd Glacier, derived from equation (3). The white contours show the ice surface elevation²⁴ at 250 m intervals.

perturbations affecting the ice–bed interface, and demonstrates that internal ice sheet mechanisms might have an important role in modulating sea level. Byrd Glacier’s period of acceleration was closely linked to the duration of lake flooding, which implies that the drainage of large and currently stable lakes (for example, Lake Vostok¹³ and the Recovery Lakes¹⁴) could make a significant and sustained change in the mass balance of large portions of Antarctica. The interaction between subglacial lakes and ice dynamics needs to be included in prognostic models of ice-sheet behaviour.

METHODS

ICE VELOCITY

Velocities are derived from automatic tracking of surface features on sequential optical images¹⁵ using a cross-correlation software package¹⁷. The measured displacements of surface features have several sources of uncertainty originating from image ortho-rectification, co-registration and application of the feature-matching technique. Ortho-rectification using a satellite-derived digital elevation model (DEM) translates the DEM errors onto the ortho-rectified image. Overall, resampling errors during ortho-projection translate to positional errors that are at the subpixel (< 15 m) level. Uncertainties associated with the image cross-correlation technique are also smaller than the nominal pixel size of 15 m. Matches with uncertainties larger than 1 pixel are discarded. The velocity errors scale with the time separation of the image pairs (see Supplementary Information, Table S1).

ELEVATION CHANGE

The data used for this study come from the Geoscience Laser Altimeter System aboard NASA’s ICESat. The Geoscience Laser Altimeter System measures surface elevation profiles along ground tracks that follow a set of reference tracks, repeating the same measurements 2 or 3 times per year. Data were selected on the basis of pulse-shape characteristics to reduce errors due to light scattering by clouds (see Supplementary Information).

We estimate temporal patterns of elevation change for small areas of the ice sheet by calculating the residuals to the plane that best fits short sections of data collected along the same reference track²⁰. We divide the reference track into overlapping 700 m segments separated by 500 m. For each segment, we fit the elevations, *z*, shot times, *t*, and return locations, *x* and *y*, with a planar model that includes a secular rate of elevation change:

$$z_p = ([x, y] - \langle [x, y] \rangle) \mathbf{m} + (t - t_0) \frac{\partial z}{\partial t} + \langle z \rangle. \tag{1}$$

Here, *m* gives the estimated surface-slope vector, $\langle [x, y] \rangle$ is the mean of the shot locations and $\langle z \rangle$ is the mean surface elevation. *t*₀ is a time close to the middle of the ICESat mission (1 December 2005), and $\partial z / \partial t$ gives the mean rate of elevation change.

The residuals to this planar model, *r* = *z* - *z*_{*p*}, give shot elevations corrected for the track separation, the surface slope and the mean rate of elevation change. The total surface displacement for each measurement is found using:

$$d\mathbf{z} = \mathbf{z} - \mathbf{z}_p + (t - t_0) \frac{\partial \mathbf{z}}{\partial t}. \tag{2}$$

Note that between equations (1) and (2), we have subtracted and added the mean rate of elevation change from the elevation measurements to calculate $\partial \mathbf{z}$. This enables the slope estimates in equation (1) to be corrected for a secular rate of elevation change, which is usually the largest component.

HYDRAULIC PRESSURE

Hydraulic pressure (*P*) is predominantly driven by surface slope and, to a lesser degree, bed topography²². We use gridded maps of ice thickness (*H*) (ref. 23) and surface elevation (*z*) (ref. 24) to solve

$$P = \rho_i g z + (\rho_w - \rho_i) g (z - H), \tag{3}$$

where *g* is gravitational potential, ρ_i is the density of ice (917 kg m⁻³) and ρ_w is the density of water (1,000 kg m⁻³). Values of *P* are derived for a 5 km grid.

The ICESat DEM (ref. 24) was scaled to 5 km to reduce noise, with an associated error of ±20 cm. Bed elevations, interpolated on the basis of radar profiles separated by up to several tens of kilometres, result in potentially large errors in the Byrd catchment region, although the ice thickness under the Byrd trunk is defined by 3 or 4 distinct profiles, and thus should be accurate to around 50 m (ref. 23). This gives a best-case hydraulic pressure difference error of the order of 5 kPa, although interpolation errors could increase this error by at least an order of magnitude.

Received 17 July 2008; accepted 20 October 2008; published 16 November 2008.

References

1. Rignot, E. J. & Thomas, R. Mass balance of polar ice sheets. *Science* **297**, 1502–1506 (2002).
2. Rignot, E. J. & Kanagaratnam, P. Changes in the velocity structure of the Greenland Ice Sheet. *Science* **311**, 986–990 (2006).
3. Joughin, I., Rignot, E., Rosanova, C. E., Lucchitta, B. K. & Bohlander, J. Timing of recent accelerations of Pine Island Glacier, Antarctica. *Geophys. Res. Lett.* **30**, L1706 (2003).
4. Stearns, L. A. & Hamilton, G. S. Rapid volume loss from two East Greenland outlet glaciers quantified using repeat stereo satellite imagery. *Geophys. Res. Lett.* **34**, L05503 (2007).
5. Shepherd, A. & Wingham, D. Recent sea-level contributions of the Antarctic and Greenland ice sheets. *Science* **315**, 1529–1532 (2007).
6. Gray, L. *et al.* Evidence for subglacial water transport in the West Antarctic Ice Sheet through three-dimensional satellite radar interferometry. *Geophys. Res. Lett.* **32**, L03501 (2005).
7. Wingham, D. J., Siegert, M. J., Shepherd, A. & Muir, A. S. Rapid discharge connects Antarctic subglacial lakes. *Nature* **440**, 1033–1036 (2006).
8. Fricker, H. A., Scambos, T. A., Bindschadler, R. & Padman, L. An active subglacial water system in West Antarctica mapped from space. *Science* **315**, 1544–1548 (2007).
9. Joughin, I. *et al.* Seasonal speedup along the western flank of the Greenland Ice Sheet. *Science* **320**, 781–783 (2008).
10. Zwally, H. J. *et al.* Surface melt-induced acceleration of Greenland Ice Sheet flow. *Science* **297**, 218–222 (2002).
11. Das, S. B. *et al.* Fracture propagation to the base of the Greenland Ice Sheet during supraglacial lake drainage. *Science* **320**, 778–781 (2008).
12. Shepherd, A., Wingham, D. & Rignot, E. J. Warm ocean is eroding West Antarctic Ice Sheet. *Geophys. Res. Lett.* **31**, L23402 (2004).
13. Siegert, M. J., Carter, S., Tabacco, I., Popov, S. & Blankenship, D. D. A revised inventory of Antarctic sub-glacial lakes. *Antarct. Sci.* **17**, 453–460 (2005).
14. Bell, R. E., Studinger, M., Shuman, C. A., Fahnestock, M. A. & Joughin, I. Large subglacial lakes in East Antarctica at the onset of fast-slowing ice streams. *Nature* **445**, 904–907 (2007).
15. Stearns, L. A. *Outlet Glacier Dynamics in East Greenland and East Antarctica*. PhD thesis, Univ. of Maine (2007).
16. Humbert, A., Greve, R. & Hutter, K. Parameter sensitivity studies for the ice flow of the Ross Ice Shelf, Antarctica. *J. Geophys. Res.* **110**, F04022 (2005).
17. Scambos, T. A., Dutkiewicz, M. J., Wilson, J. C. & Bindschadler, R. A. Application of image cross-correlation to the measurement of glacier velocity using satellite image data. *Remote Sens. Environ.* **42**, 177–186 (1992).
18. Swinbank, C. W. Ice movement of valley glaciers flowing into the Ross Ice Shelf, Antarctica. *Science* **141**, 523–525 (1963).
19. Brecher, H. Photographic determination of surface velocities and elevations on Byrd Glacier. *Antarct. J. US* **17**, 79–81 (1982).
20. Howat, I. M., Smith, B. E., Joughin, I. & Scambos, T. A. Rates of southeast Greenland ice volume loss from combined ICESat and ASTER observations. *Geophys. Res. Lett.* **35**, L17505 (2008).
21. Sergienko, O. V., MacAyeal, D. R. & Bindschadler, R. A. Causes of sudden, short-term changes in ice-stream surface elevation. *Geophys. Res. Lett.* **34**, L22503 (2007).
22. Shreve, R. L. Movement of water in glaciers. *J. Glaciol.* **11**, 205–214 (1972).
23. Lythe, M. B. & Vaughan, D. G. BEDMAP: A new ice thickness and subglacial topographic model of Antarctica. *J. Geophys. Res.* **106**, B6 (2001).

24. DiMarzio, J. A., Brenner, A., Schutz, R., Shuman, C. A. & Zwally, H. J. *GLAS/ICESat 1 km Laser Altimetry Digital Elevation Model of Greenland* (National Snow and Ice Data Center, 2007).
25. Kamb, B. Glacier surge mechanism based on linked cavity configuration of the basal water system. *J. Geophys. Res.* **92**, 469–479 (1987).
26. Whillans, I. M., Chen, Y. H., Van der Veen, C. J. & Hughes, T. J. Force budget: III. Application to the three-dimensional flow of Byrd Glacier, Antarctica. *J. Glaciol.* **35**, 68–80 (1989).
27. Drewey, D. *Antarctica: Glaciological and Geophysical Folio* (Univ. of Cambridge, Geophysical folio, 1983).
28. Scambos, T. A., Haran, T. M., Fahnestock, M. A., Painter, T. H. & Bohlander, J. MODIS-based Mosaic of Antarctica (MOA) data sets: Continent-wide surface morphology and snow grain size. *Remote Sens. Environ.* **111**, 2–3 (2007).

Supplementary Information accompanies the paper at www.nature.com/naturegeoscience.

Acknowledgements

We thank C. Swithinbank for providing raw data and maps from his 1961 Antarctic field season. B. Lucchitta and T. Hughes provided us with Landsat TM4 scenes of Byrd Glacier. SPOT images are courtesy of the CNES/SPIRIT program. Research was supported by a NASA ESS fellowship (NNG05-GQ3H) to L.A.S., NSF grant ANT-0636719 to B.E.S. and NASA grant NNG04-GK39G to G.S.H.

Author contributions

All authors contributed equally to the manuscript, and approve the version being submitted.

Author information

Reprints and permissions information is available online at <http://npg.nature.com/reprintsandpermissions>. Correspondence and requests for materials should be addressed to L.A.S.